AJNR

Perineural spread of head and neck tumors: how accurate is MR imaging?

W R Nemzek, S Hecht, R Gandour-Edwards, P Donald and K McKennan

AJNR Am J Neuroradiol 1998, 19 (4) 701-706
http://www.ajnr.org/content/19/4/701

AJNR Am J Neuroradiol 19:701–706, April 1998

Perineural Spread of Head and Neck Tumors: How Accurate Is MR Imaging?

William R. Nemzek, Stephen Hecht, Regina Gandour-Edwards, Paul Donald, and Kevin McKennan

PURPOSE: **Our aim was to determine the precision of MR imaging evaluation of perineural spread of head and neck tumors.**

METHODS: **Nineteen patients had complete extirpation of head and neck tumors (10 squamous cell carcinomas, four adenoid cystic carcinomas, one poorly differentiated carcinoma, one salivary duct carcinoma, one mucoepidermoid carcinoma, one chordoma, and one meningioma) with histologic confirmation of perineural spread. Findings at presurgical contrast-enhanced MR imaging were compared with findings at pathologic examination.**

RESULTS: **The sensitivity of MR imaging for detection of perineural spread was 95%; however, the sensitivity for mapping the entire extent of perineural spread fell to 63%.**

CONCLUSION: **MR imaging may fail to depict microscopic foci of perineural tumor infiltration, leading to underestimation of the extent of perineural spread. Nevertheless, with careful analysis of foraminal architecture and MR enhancement patterns, one can reliably identify the presence if not the extent of perineural spread.**

Perineural invasion is one of the most treacherous and insidious forms of tumor spread and is a nightmare for the radiologist and the surgeon. Because of the extensive neural system, malignant tumors of the head and neck have many avenues by which to invade cranial nerves and gain entrance to intracranial structures (1, 2).

Most of the lesions in this study were treated with skull base surgery—a multidisciplinary field combining the talents of head and neck surgeons, otologists, neurosurgeons, plastic surgeons, pathologists, and radiologists. Lesions that extend through the skull base, previously considered incurable and amenable only to palliative therapy, are now approached surgically and removed completely (3–5). The skull base surgeon must rely on clinical assessment, imaging studies, and the liberal use of fine-needle aspiration biopsy preoperatively and frozen section diagnosis during surgery for tumor localization and mapping. Radiologic staging is critical for determining resectability and for planning the surgical approach.

Perineural spread has a significant, negative impact on treatment and prognosis, because it requires more extensive surgical resection and adversely affects treatment outcome. Patients who have perineural spread often have tumor recurrence, and long-term survival is jeopardized. Many treatment failures are related to unrecognized perineural tumor invasion (6–8).

The purpose of our study was to evaluate the accuracy of MR imaging in detecting the perineural spread of tumor and in mapping its extent.

Methods

Between August 1990 and December 1996 we evaluated 65 patients with pathologic confirmation of perineural invasion. Patients with histologic evidence of perineural tumor in nerves restricted to the bulk of the primary tumor mass and those who had no preoperative MR imaging were excluded from the study. Inoperable lesions or tumors that were treated with radiation, such as lymphomas, were also excluded. The study group included only patients with tumor demonstrated pathologically as having spread beyond the location of the primary tumor along the neural structures. In order to determine the extent of perineural disease, we included in the study only those patients who were candidates for complete removal of their tumor.

These selection criteria yielded a group of 19 patients whose imaging, pathologic, and surgical findings were reviewed retrospectively (see Table). There were seven women and 12 men, ranging in age from 28 to 68 years (mean age, 55 years).

Because we are a tertiary referral center, MR images were obtained with a variety of imaging units and protocols. MR examinations were performed on a 1.5-T magnet (with one exception, in which a 0.3-T magnet was used) and included sagittal and axial T1- and T2-weighted studies. T1-weighted

Received April 24, 1997; accepted after revision October 1.

From the Departments of Radiology (W.R.N., S.H.), Pathology (R.G-E.), and Otolaryngology (P.D.), University of California Davis Medical Center, Sacramento, Calif; and Sacramento Ear, Nose and Throat, Sacramento, Calif (K.McK.).

Address reprint requests to William R. Nemzek, MD, University of California Davis Medical Center, 2516 Stockton Blvd, TICON II, Room 216, Sacramento, CA 95817.

Pathologic radiologic correlation in 19 patients with perineural spread of head and neck tumors

Case	Age, y/Sex	Histologic Diagnosis	Primary Site	Cranial Nerves with Pathologically Proved Perineural Spread	MR Findings	Detection/Extent of Spread*
1	49/M	Adenoid cystic ca	Nasal cavity	II, III, IV, V2	CE, CS, SOF, apex orbit	Y/Y
2	66/F	Adenoid cystic ca	Parotid	VII	CE, mastoid segment VII (enlarged) (false-negative tympanic segment)	Y/N
3	42/F	Adenoid cystic ca	Nasopharynx	V3, V	CE, CS, SOF, Meckel cave	Y/N
4	28/F	Adenoid cystic ca	Nasopharynx	III, V, V2, ION, VI, IX, X, XI, XII	CE, hypoglossal foramen, CS, jugular fossa, PPF	Y/N
5	53/F	Chordoma	Clivus	IX, X, XI, XII	CE, jugular fossa, hypoglossal foramen (enlarged)	Y/Y
6	50/M	Meningioma, atypical	Middle fossa	V	CE, CS Meckel cave	Y/Y
7	66/F	Mucoepidermoid ca	Parotid	VII	CE, IAC	Y/Y
8	42/M	Poorly differentiated ca	Nasopharynx	V1, III, IV, VI	CE, SOF, CS, Meckel cave	Y/Y
9	71/F	Salivary duct ca	Parotid	V3	False-negative	N/N
10	60/M	Squamous cell ca	Maxillary sinus	ION	CE, ION	Y/Y
11	53/M	Squamous cell ca	Maxillary sinus	V2	CE, PPF	Y/Y
12	58/M	Squamous cell ca	Nasopharynx	V3, XII	CE, foramen ovale, hypoglossal foramen	Y/Y
13	50/M	Squamous cell ca	Nasal cavity	V3, V	CE, foramen ovale, Meckel cave	YY
14	64/M	Squamous cell ca	Retromolar Trigone	V2, V	CE, CS, foramen ovale	Y/N; False-positive at foramen ovale
15	54/M	Squamous cell ca	Nasopharynx	V	CE, CS, SOF, Meckel cave	Y/Y
16	61/M	Squamous cell ca	Eyelid, inf	ION	CE, ION	Y/N
17	62/M	Squamous cell ca	Ethmoid, max sinus	V2	CE, PPF	Y/Y
18	68/F	Squamous cell ca	Forehead, skin	III, IV, V, V2, VI, ION	CE, CS	Y/N
19	53/M	Squamous cell ca	Retromolar Trigone	V3	CE, foramen ovale	Y/Y

Note.—ca indicates carcinoma; CE, contrast enhancement; ION, infraorbital nerve; CS, cavernous sinus; SOF, superior orbital fissure; IAC, initial auditory canal; PPF, pterygopalatine fossa; Y, yes; N, no.

* Pathologic demonstration of entire extent of perineural spread.

coronal and/or axial 3- to 5-mm-thick images were repeated after the infusion of gadopentetate dimeglumine (0.1 mmol/kg). Two radiologists analyzed the images.

MR imaging signs of perineural spread include enhancement of the neural foramen, or Meckel's cave, enlargement of the nerve or cavernous sinus, or enhancement of the individual nerve. The neural foramen or nerve may be enlarged.

Initially, the entire course of each nerve traversing the primary tumor site was evaluated in both anterograde and retrograde directions. For example, the pathway of V2 was followed from the infraorbital nerve through the pterygopalatine fossa, foramen rotundum, cavernous sinus, Meckel's cave, and cisternal segment of the trigeminal nerve to the pons. If an abnormality was encountered at the junction of several cranial nerves—for example, in the cavernous sinus—then the pathways of all the cranial nerves in the cavernous sinus were scrutinized. Once the bulk of the tumor was removed, multiple frozen sections were taken and immediately interpreted by the pathologist until tumor-free margins were obtained.

Results

The most common tumor associated with perineural spread was squamous cell carcinoma (n = 10), followed by adenoid cystic carcinoma (n = 4) (Table).

The trigeminal nerve and its branches were involved in 16 patients. The trigeminal nerve was affected in Meckel's cave in five cases and in the cavernous sinus in seven patients. The ophthalmic division (V1) was involved in one case, the maxillary division (V2) in six, and the mandibular division (V3) in five. The infraorbital nerve was involved in four patients. There was perineural spread in the hypoglossal (XII) and trochlear nerves in three patients and in the oculomotor and abducens nerves (III and VI) in four cases. The facial, glossopharyngeal, vagus, and spinal accessory nerves (VII, IX, X, and XI, respectively) were each involved twice, and cranial nerve II was involved once (see Table).

MR imaging correctly depicted the presence of perineural spread of disease in all cases except one. The sensitivity for detection was 95%; however, the entire extent of disease was predicted accurately in 12 of 19 cases, yielding a sensitivity of 63% for complete accurate mapping of perineural spread. The sample is skewed to include only patients who had histologically proved perineural spread, so specificity cannot be measured accurately.

In two cases, enlargement and enhancement of the infraorbital nerve was seen only at the infraorbital foramen, but tumor was present throughout the entire course of the nerve (Figs 1 and 2; case 16, 4). Figure 1 shows scattered nests of tumor cells in the infraorbital nerve at the pterygopalatine fossa.

Perineural spread occurs both retrogradely and an-

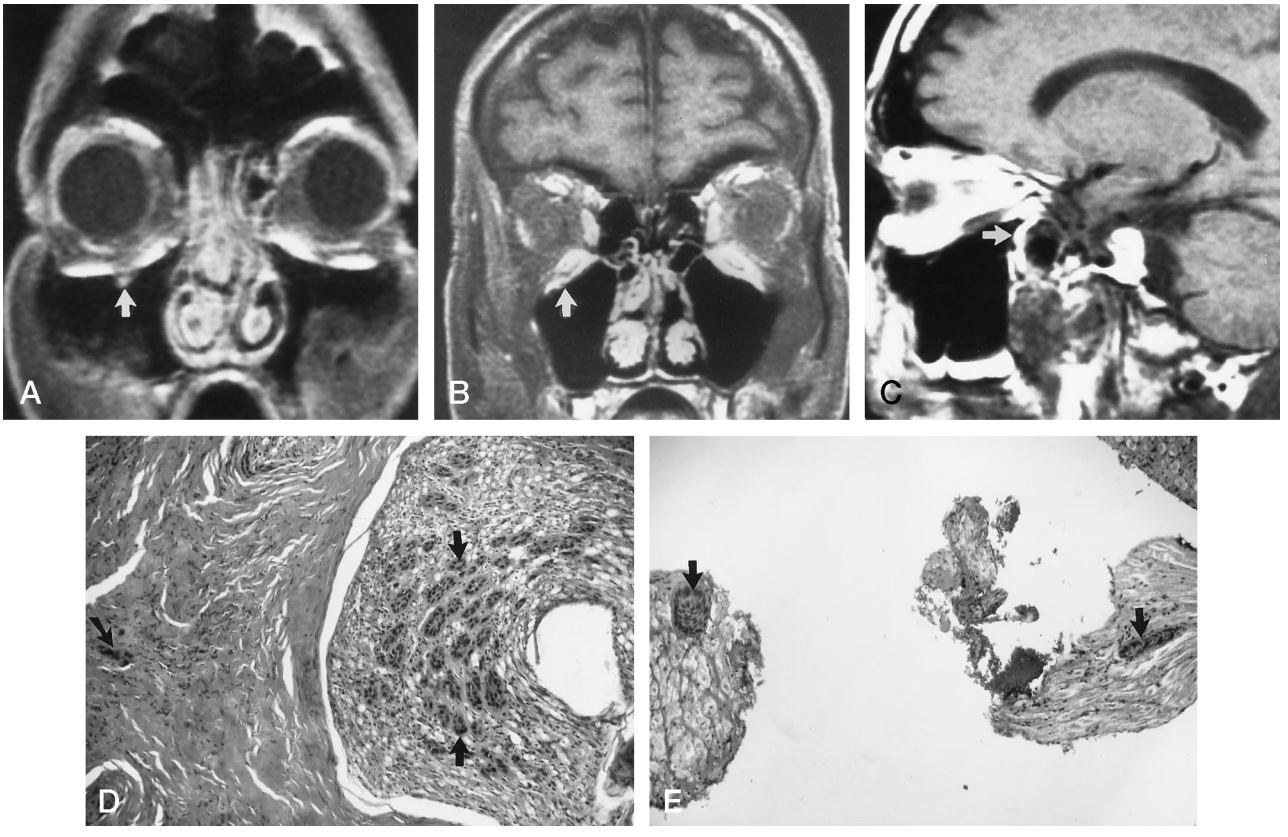

FIG 1. Case 16: Squamous cell carcinoma of the lower eyelid in a 61-year-old man with retrograde perineural spread along the infraorbital nerve.

A, T1-weighted contrast-enhanced coronal MR image with fat saturation shows enhancement of an enlarged right infraorbital nerve (*arrow*).

B, T1-weighted contrast-enhanced coronal MR image posterior to *B* shows the infraorbital nerve is of normal size and does not enhance (*arrow*).

C, T1-weighted noncontrast sagittal MR image shows a normal fat-filled pterygopalatine fossa (*arrow*).

D, Histologic section of the infraorbital nerve at the infraorbital foramen shows perineural and extensive endoneural infiltration by tumor (*arrows*).

E, Histologic section at the pterygopalatine fossa shows only scattered nests of tumor cells (*arrows*).

FIG 2. Case 4: Adenoid cystic carcinoma arising in the nasopharynx in a 28-year-old woman with anterograde spread along the entire infraorbital nerve.

A, T1-weighted contrast-enhanced axial MR image reveals tumor growing into the occipital bone and through the left jugular fossa (*straight solid arrow*). There is destruction of the pterygoid process of the sphenoid (*open arrow*) and minimal invasion of the left pterygopalatine fossa (*curved arrow*). Note normal fatty marrow in right pterygoid process.

B, T1-weighted contrast-enhanced coronal MR image shows enlargement and enhancement to the infraorbital nerve near the infraorbital foramen (*arrow*).

C, The infraorbital nerve is normal posterior to *A* (*arrow*).

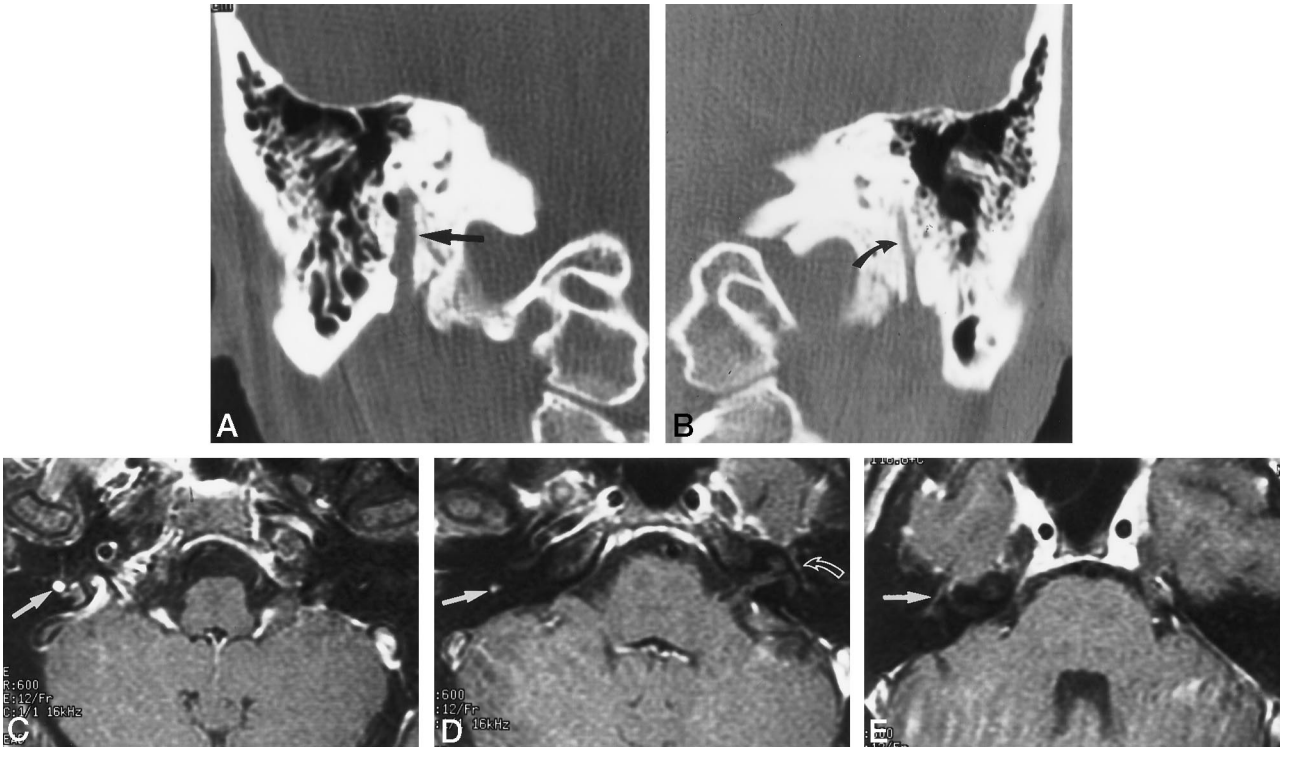

FIG 3. Case 2: Adenoid cystic carcinoma from the parotid in a 66-year-old woman with facial nerve palsy. Perineural spread extends to level of the geniculate ganglion.

A, Coronal CT scan shows enlargement and erosion of the mastoid segment of the right facial nerve canal (*arrow*). Reproduced with permission from Barnes et al (24).

B, Normal left side for comparison (*curved arrow*).

C, T1-weighted contrast-enhanced MR image shows enlarged enhancing mastoid segment of the facial nerve (*arrow*). Reproduced with permission from Barnes et al (24).

D, T1-weighted contrast-enhanced MR image superior to *C* shows the right facial nerve is enlarged and enhancing at the level of the posterior genu (*straight arrow*). There is minimal enhancement of the normal tympanic segment of the contralateral facial nerve (*curved arrow*).

E, T1-weighted contrast-enhanced MR image superior to *D*. Enhancement of the tympanic segment (*arrow*) and the geniculate portion of the right facial nerve was interpreted as normal. Nests of tumor cells were found throughout the tympanic segment of the facial nerve 5 mm from the geniculate ganglion.

terogradely. In case four (adenoid cystic carcinoma arising from the nasopharynx), perineural spread was depicted accurately in the cavernous sinus, jugular fossa, hypoglossal foramen, and pterygopalatine fossa. The extent of the anterograde spread of tumor along the entire course of the infraorbital nerve was not identified. The midsection of the nerve appeared normal, but enlargement and enhancement was noted near the infraorbital foramen (Fig 2). This was considered to be an example of incomplete tumor estimation.

Spread of adenoid cystic carcinoma was detected histologically along the course of the facial nerve from the parotid gland to just proximal to the geniculate ganglion. On MR images, facial nerve involvement was detected in the mastoid segment but was not apparent in the tympanic segment of the nerve (Fig 3).

In a case of salivary duct carcinoma of the parotid gland (Fig 4), tumor extended centrifugally along the proximal inferior alveolar nerve through the mandibular foramen. The T1-weighted MR sequences showed decreased signal of the normal mandibular marrow, which represented edema, but did not show discrete enhancement along the course of the nerve. CT scans, however, showed erosion of the lingula and replacement of normal fat at the mandibular foramen.

In the single MR examination performed on a 0.3-T magnet, cavernous sinus involvement was seen, but there was no enhancement of the abnormal infraorbital nerve. The one false-positive MR finding was enhancement of the foramen ovale (case 14), but at pathologic examination, only the periosteum was involved.

Discussion

Because 30% to 45% of patients with perineural invasion are initially asymptomatic (9), the radiologist has a crucial role in detecting subclinical spread of disease. The strengths and limitations of the available imaging techniques must be understood to provide optimum benefit to patients and clinical colleagues.

The patients in this study represented an ideal group by which to evaluate the extent of perineural spread, because in the quest for complete tumor removal, the surgeon attempts to obtain a tumor-free

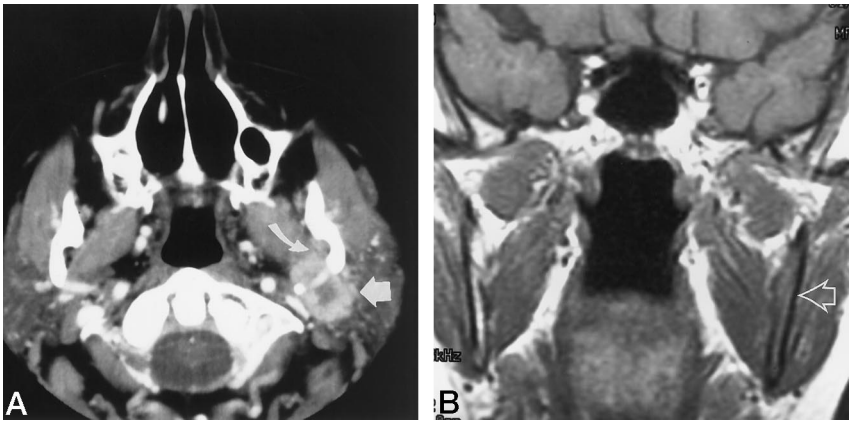

FIG 4. Case 9: Salivary duct carcinoma in a 71-year-old woman with anterograde perineural spread along the proximal inferior alveolar nerve through the mandibular foramen.

A, Axial contrast-enhanced CT scan shows an enhancing mass arising in the parotid (*straight arrow*) and extending into the medial pterygoid muscle and the mandibular foramen. Note enlargement of the mandibular foramen with replacement of normal fat and erosion of lingula (*curved arrow*). Compare with opposite mandibular foramen containing normal fat. Reproduced with permission from Nemzek et al (25).

B, Coronal noncontrast T1-weighted MR image shows diffuse abnormal signal of the marrow of the ramus of the mandible (*arrow*). No perineural enhancement was identified (not shown).

margin. Thus, the extent of perineural spread of tumor is documented.

Nerves act as conduits that transmit tumor from a primary site to a deeper structure. Head and neck cancers can leave the primary tumor mass and travel retrogradely along nerves to reemerge at deeper intracranial destinations (1). Cranial nerves V and VII are most commonly involved because of their extensive distribution (9). Once tumors reach the cavernous sinus, additional cranial nerves may be involved, particularly the oculomotor system (9). Perineural spread of malignancy occurs by both centripetal and centrifugal growth. Once tumor reaches a branch point in a nerve or is contiguous with another nerve, perineural spread may track both proximally and distally (9, 10). MR imaging evidence of anterograde spread of tumor must be diligently sought after as well (Figs 2 and 4).

It is important to distinguish between perineural invasion and perineural spread. Perineural invasion is a pathologic term that describes microscopic perineural or endoneural tumor. This histologic finding has grave prognostic implications. Perineural invasion is often confined to the main tumor mass and is impossible to detect radiologically. Perineural spread of malignancy describes the process by which a tumor exits its primary site and reaches distant locations by traveling along the neural sheath. Perineural spread is defined as separate from the main bulk of the tumor.

Our study group included a single benign tumor, an atypical meningioma (case 6), in which there was no invasion of the perineurium or endoneurium, as is seen with malignancy. However, there was extensive perineural spread around the mandibular branch of the trigeminal nerve, extending into the foramen ovale. Since the meningioma was using V3 as a scaffolding and a path of exit from its primary site, this qualified as perineural spread of this benign tumor.

Neurons themselves are resistant to tumor. Tumors gaining a foothold in the coverings of a nerve attain a pathway for invasion. As tumor accumulates, the nerve enlarges, producing concentric enlargement and erosion of the foramina through which it passes. The imaging signs of perineural spread include foraminal enlargement and replacement of normal fat within neural foramina. Contrast-enhanced MR images show enhancement of the nerve, which cannot be imaged with CT (2, 11).

Portions of the facial nerve normally enhance on temporal bone MR images in the regions of the proximal greater superficial petrosal nerve, the geniculate ganglion, and the tympanic (Fig 3D) and mastoid segments (12, 13). Areas of normal neural enhancement may mask the pathologic neural enhancement, complicating the detection of perineural spread (Fig 3). Only enlargement of the facial nerve can be used as a reliable indicator of tumor at this location, because of native enhancement.

The blood-nerve barrier is maintained by the combined action of the endothelium of endoneural capillaries and an inner perineurium (14–17). The perineurium is a cellular layer that invests each nerve fascicle. Nerve injury has a biphasic response marked initially by endoneural vascular permeability and later by perineurial breakdown (14, 15, 17, 18). Various mechanisms for the enhancement of nerves include inflammation, demyelination, ischemia, trauma, and axonal degeneration (11, 12, 17, 19). These insults may disrupt the blood-nerve barrier, allowing leakage and accumulation of contrast material. The geniculate, tympanic, and mastoid segments of the facial nerve are like peripheral nerves, possessing peri- and epineural venous plexus. Congestion of the epineural and perineural venous plexus may cause enhancement by an increased vascular pool of contrast material (12, 15, 17). With current imaging techniques, we can detect gross tumor spread that has disrupted the internal milieu of the nerve. Perineural enhancement may depend on extensive destruction of the barrier functions of the intraneural microvascular circulation and the perineurium. MR imaging may fail to detect more subtle scattered microscopic nests of tumor cells that represent the true front of advancing tumor invasion.

Intracranial extension of nasopharyngeal carcinoma is often thought to enter the cranial vault via

the foramen lacerum or foramen ovale. This is often associated with gross tumor extension with erosion of the skull base and not perineural invasion (8). Note that in one of our patients there was enhancement of the foramen ovale but no histologic evidence of perineural invasion. A bulky tumor mass, contiguous with the foramen ovale, produced the enhancement, but no tumor was found at surgery in this location.

"Skip lesions" are also known to occur in both squamous cell and basal cell carcinoma (20, 21). In our series, continuous perineural involvement of the nerve was histologically proved in all cases. In two cases, MR imaging failed to show the perineural invasion in contiguity, but there was evidence of abnormal enhancement distally. The amount of tumor burden can be variable along the course of a nerve: regions with relatively little tumor can fail to enhance. Therefore, the entire course of the nerve must be scrutinized to avoid underestimation of perineural spread (Fig 2).

In our series, fat saturation was used on T1-weighted images, because it was thought that it would improve detection of subtle contrast enhancement of the infraorbital nerve; however, this technique must be used judiciously, as it may introduce magnetic susceptibility artifacts at air/soft-tissue interfaces and obscure disease (Fig 1). Very high doses of contrast material (17) may enhance the ability to detect perineural disease, as has been proved in the imaging of intracranial metastases (22, 23).

Conclusion

MR imaging may fail to depict microscopic foci of perineural tumor infiltration and underestimate the extent of perineural invasion. Normal neural enhancement, such as along the tympanic segment of the facial nerve, may mask perineural spread of tumor. Attention to detail, with thorough knowledge of anatomy and of the pathways of perineural spread, a meticulous thin-section contrast-enhanced MR imaging technique, and judicious use of fat saturation are essential. Nevertheless, careful analysis of foraminal architecture and MR enhancement patterns will detect most perineural spread.

Acknowledgment

We thank Kathy Sommers for invaluable help in preparing this manuscript.

References

1. Curtin HD, Williams RW, Johnson J. **CT of perineural tumor extension: pterygopalatine fossa.** *AJNR Am J Neuroradiol* 1984;5: 731–737
2. Laine F, Braun IF, Jensen ME, Nadel L, Som PM. **Perineural tumor extension through the foramen ovale: evaluation with MR imaging.** *Radiology* 1990;174:65–71
3. Donald P. **Skull base surgery.** *Otolaryngol Head Neck Surg* 1992; 106:10–11
4. Ojeman R. **Skull base surgery: a perspective (guest editorial).** *J Neurosurg* 1992;76:569–570
5. Pensak M. **Skull base surgery issues (editorial).** *Ear Nose Throat J* 1991;70:673–674
6. Eisen MD, Yousem DM, Motone KT, et al. **Use of preoperative MR to predict dural, perineural, and venous invasion of skull base tumors.** *AJNR Am J Neuroradiol* 1996;17:1937–1945
7. Frankenthaler RA, Luna MA, Lee SS, et al. **Prognostic variables in parotid gland cancer.** *Arch Otolaryngol Head Neck Surg* 1991;117: 1251–1256
8. Sham JST, Cheung YK, Choy D, Chan FL, Leong L. **Cranial nerve involvement and base of skull erosion in nasopharyngeal carcinoma.** *Cancer* 1991;68:422–426
9. Catalano PJ, Sen C, Biller HF. **Cranial neuropathy secondary to perineural spread of cutaneous malignancies.** *Am J Otol* 1995;16: 772–777
10. Carter RL, Foster CS, Dinsdale EA, Pittam MR. **Perineural spread by squamous cell carcinomas of the head and neck: a morphological study using antiaxonal and antimylin monoclonal antibodies.** *J Clin Pathol* 1983;36:269–275
11. Hudgins P. **Contrast enhancement in head and neck imaging.** *Neuroimaging Clin N Am* 1994;4:101–115
12. Sartoretti-Schefer S, Wichmann W, Valavanis A. **Idiopathic, herpetic and HIV-associated facial nerve palsies: abnormal MR enhancement patterns.** *AJNR Am J Neuroradiol* 1994;15:479–485
13. Gebarski SS, Telian SA, Niparo JK. **Enhancement along the normal facial nerve in the facial canal: MR imaging and anatomic correlation.** *Radiology* 1992;183:391–394
14. Latker CH, Wadhwani KC, Balbo A, Rapoport SI. **Blood-nerve barrier in the frog during wallerian degeneration: are axons necessary for the maintenance of barrier function?** *J Comp Neurol* 1991;380:650–664
15. Lundberg G. **Structure and function of the intraneural microvessels as related to trauma, edema formation and nerve function.** *J Bone Joint Surg* 1975;57A:938–948
16. Kobayashi S, Yoshizawa H, Hachiya Y, Ukai T, Morita T. **Vasogenic edema induced by compression injury to the spinal nerve root: distribution of intravenously injected protein tracers and gadolinium-enhanced magnetic resonance imaging.** *Spine* 1993;18: 1410–1424
17. Sartoretti-Schefer S, Brändle P, Wichmann W, Valvanis A. **Intensity of contrast enhancement does not correspond to clinical and electroneurographic findings in acute inflammatory facial nerve palsy.** *AJNR Am J Neuroradiol* 1996;17:1229–1236
18. Sparrow JR, Kiernan JA. **Endoneural vascular permeability in degenerating and regenerating peripheral nerves.** *Acta Neuropathol* 1981;53:181–188
19. Jinkins J. **Magnetic resonance imaging of benign nerve root enhancement in the unoperated and postoperative lumbosacral spine.** *Neuroimaging Clin N Am* 1993;3:525–541
20. Carlson KC, Roenigk RK. **Know your anatomy: perineural involvement of basal and squamous cell carcinoma of the face.** *J Dermatol Surg Oncol* 1990;9:827–833
21. Hanke CW, Wolf WR, Hochman SA, O'Brian JJ. **Chemosurgical reports: perineural spread of basal cell carcinoma.** *J Dermatol Surg Oncol* 1983;9:742–747
22. Schaefer PW, Budzik RF, Gonzalez RG. **Imaging of cerebral metastases.** *Neurosurg Clin N Am* 1996;7:393–423
23. Haustein J, Laniado M, Niendorf HP, et al. **Triple-dose versus standard-dose gadopentetate dimeglumine: a randomized study in 199 patients.** *Radiology* 1993;186:855–860
24. Barnes L, Kapadia SB, Nemzek WR, Weissman JL, Janecka IP. **Biology of selected skull base tumors.** In: Janecka IP, Tiedemann K, eds. *Skull Base Surgery, Anatomy, Biology, and Technology.* Philadelphia, Pa: Lippincott-Raven; 1997:263–289
25. Nemzek WR. **The trigeminal nerve.** ***Top Magn Reson Imaging*** 1996; 8:132–154